Available online at www.sciencedirect.com
SCIENCE DIRECT®
Chemical Physics Letters 389 (2004) 140–144
CHEMICAL PHYSICS LETTERS
www.elsevier.com/locate/cplett

Spiral wave dynamics controlled by a square-shaped sensory domain

On-Uma Kheowan [a,*], Supichai Kantrasiri [a], Chananate Uthaisar [a], Vilmos Gáspár [b], Stefan C. Müller [c]

[a] Department of Chemistry, Mahidol University, Rama 6 Road, Bangkok 10400, Thailand
[b] Institute of Physical Chemistry, University of Debrecen, P.O. Box 7, H-4010 Debrecen, Hungary
[c] Institut für Experimentelle Physik, Otto-von-Guericke-Universität, Universitätsplatz 2, D-39106 Magdeburg, Germany

Received 6 February 2004; in final form 17 March 2004

Abstract

Spiral waves rotating rigidly in a thin layer of the light-sensitive Belousov–Zhabotinsky (BZ) reaction are subjected to a time-dependent uniform illumination. A non-local feedback algorithm computes the illumination intensity to be proportional to the average wave activity within a square-shaped sensory domain. The investigations show a broad spectrum of dynamical responses which results in square- and cross-shaped trajectories of the spiral tip, including reflections at the virtual walls. The geometry of the sensory domain is crucial in determining size and shape of the tip trajectories. A theoretical approach is proposed to explain the observed phenomena.

Controlling the evolution of complex processes in time and space is a major research issue of nonlinear dynamics [1,2]. It is important for many dynamical phenomena including the formation of spatio-temporal patterns in chemical reactions like the CO oxidation on platinum surfaces [3,4] or the Belousov–Zhabotinsky (BZ) reaction [5,6]. Some of the effective control methods have been applied to chemical waves propagating in excitable media, such as external (periodic) forcing [7–9]. Methods involving a time-delayed feedback [2], require more complex algorithms [10,11] that are based on collecting data on the activity level of the medium.

In this report we investigate spiral waves rotating in an excitable layer of the BZ reaction. The activity level in this medium can be measured at one point (local feedback) [9,12], in a given domain (non-local feedback) [13,14] and at all points (global feedback) [10]. Of both theoretical and practical interest is the effect of shape and size of the applied 'sensory domain' on the dynamics of rotating spiral waves under feedback control. We apply square-shaped domains and find a broad spectrum of dynamical responses, including square-shaped and cross-shaped trajectories of the spiral tip. Numerical simulations using the light-sensitive Oregonator model [15,16] reproduce this behaviour. We suggest that the feedback method introduced in this work offers an efficient tool for controlling also the dynamics of other excitable media.

We study spiral wave dynamics in thin layers of the BZ reaction with the light-sensitive $Ru(bpy)_3^{2+}$ catalyst [17]. This catalyst promotes the autocatalytic production of $HBrO_2$, the activator species of the BZ system. The applied illumination enhances the production of the bromide ion, an inhibitor species, and thus decreases the system's excitability which, in turn, results in slowing down the wave activity in the medium. This provides an experimentally accessible method to control spiral wave dynamics, in that the light intensity influences parameters such as the wavelength and the diameter of the spiral core.

In our experiments, the $Ru(bpy)_3^{2+}$ catalyst was immobilized in a silica gel matrix [18] (thickness 0.3 mm, diameter 5 cm) at a concentration of 4.2 mM. The reactants and their concentrations (disregarding bromination of malonic acid) were: $NaBrO_3$ (0.20 M), malonic acid (0.17 M), H_2SO_4 (0.39 M) and NaBr (0.09 M) [12]. The experiments were carried out at an ambient

* Corresponding author. Fax: +662-2458332.
E-mail address: scokw@mucc.mahidol.ac.th (O.-U. Kheowan).

0009-2614/$ - see front matter © 2004 Elsevier B.V. All rights reserved.
doi:10.1016/j.cplett.2004.03.077

temperature of 25 ± 1 °C. We created a spiral wave by using a spot (diameter, 1 cm) of intense light from a cold light source to break a propagating wave front (this creates two wave ends) and suppressing one of the open ends with the light spot to leave a single spiral in the center of the dish [12]. The reaction layer was uniformly illuminated from below with a video projector controlled by a computer via a frame grabber. The oxidation waves were observed in transmitted light by a CCD camera and stored on a computer. The main features of spiral rotation, the trajectory of spiral tip, is determined by a special computer procedure given in [9].

In our non-local feedback algorithm, the illumination intensity applied to the reaction layer is given by Kheowan et al. [13]

$$I(t) = I_0 + k_{\mathrm{fb}}[B(t) - B_0], \tag{1}$$

where I_0 is a constant background intensity. $B(t)$ is the average grey level of the pixels in the square-shaped sensory domain

$$B(t) = \frac{1}{n}\sum_{i=1}^{n} G_i(t), \tag{2}$$

where $0 \leqslant G_i \leqslant 255$ is the grey level of a given pixel, and n is the total number of pixels in the domain. Note that a larger grey level corresponds to higher concentration of the oxidized form of the catalyst (bright fronts). The intensity of the feedback illumination $I(t)$ is controlled by the gain k_{fb}, and the value of $B(t)$. The constant B_0 is the $B(t)$ averaged over one period of a spiral placed in the center of the square domain and illuminated with background intensity I_0.

The effects of such non-local feedback on a rigidly rotating spiral wave are shown in Fig. 1. For a side length d of the domain significantly smaller than the spiral wavelength λ ($d = 0.5\lambda$), the spiral leaves the center of the sensory domain, where its circular core was initially placed (arrow in Fig. 1a), by drifting outwards until it makes a turn to follow a circular path with a radius of about 0.76λ. This motion resembles that observed in earlier reported experiments applying a small size, circular-shaped sensory domain [13].

For a domain size equal to the spiral wavelength ($d = \lambda$), the spiral core first drifts away from the domain center (Fig. 1b), then it approaches a stable, square-shaped trajectory with a side length of about 1.33λ, which is rotated by about 45° with respect to the domain. Note that the drift velocity of the spiral wave core changes periodically: it is slower at the corners and faster at the sides of the trajectory.

Fig. 1c shows the trajectory of the spiral tip in an experiment with a still larger feedback domain, $d = 1.25\lambda$. In this case, the spiral tip was initially placed close to the domain boundary. The feedback control induces first a drift towards the center and subsequently towards the middle region of the adjacent side of the domain. This process occurs several times and consequently the spiral tip is caught inside the square, bouncing from and to the 'virtual walls'. Fig. 1a–c indicate that increasing the size d of the feedback domain has a pronounced effect on the shape and size of the spiral tip trajectory. In certain ranges of increasing d, the size of the square trajectory is reduced. Experiments also show that the trajectories act like attractors: the spiral tip always approaches them independently from its initial position.

We complemented the experiments by numerical simulations using the Oregonator model [15], extended by a term $\phi = \phi(t)$ accounting for the effect of bromide ion produced due to the illumination [16]:

$$\frac{\partial u}{\partial t} = \frac{1}{\epsilon}\left[u - u^2 - (fv + \phi)\frac{u - q}{u + q}\right] + \nabla^2 u, \tag{3}$$

$$\frac{\partial v}{\partial t} = u - v. \tag{4}$$

Here, the variables u and v describe the evolution of the concentration of the autocatalytic species $HBrO_2$ and

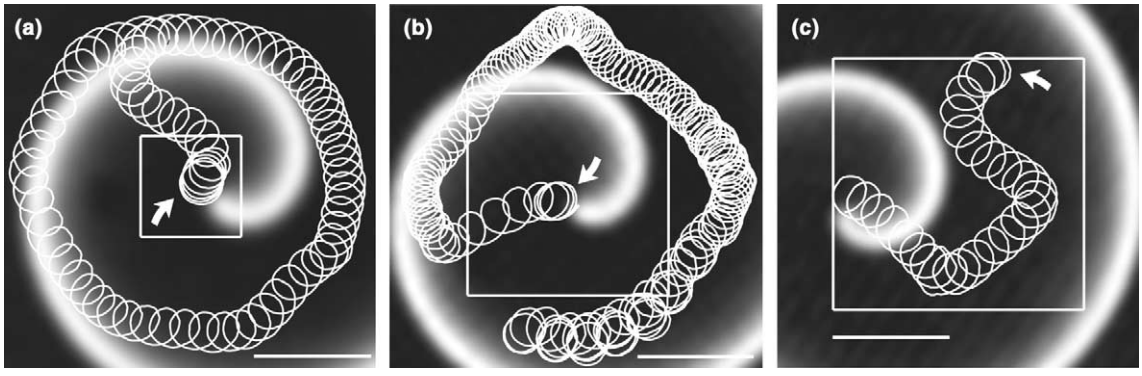

Fig. 1. Experimental trajectories of a spiral wave tip subjected to the feedback control Eqs. (1) and (2) for different sizes of the sensory domain: (a) $d = 0.5\lambda$ (λ = spiral wavelength) with $B_0 = 24$, $k_{\mathrm{fb}} = 0.2$, (b) $d = 1.0\lambda$ with $B_0 = 24.5$, $k_{\mathrm{fb}} = 0.8$, and (c) $d = 1.25\lambda$ with $B_0 = 19$, $k_{\mathrm{fb}} = 0.45$. $I_0 = 0.70$ mW cm^2 for all experiments. The domains and the initial spiral core locations are indicated by squares and thick arrows, respectively. The spiral images are shown for the start of the trajectory in (a) and (b) and the end of the trajectory in (c). Scale bar: 1 mm.

the oxidized form of the catalyst, respectively. Due to the immobilization of the catalyst, variable v does not diffuse in this model. The parameters $\varepsilon = 0.05$, $q = 0.002$ and $f = 3.5$ are kept constant. Non-local feedback is introduced into the model by varying the value of $\phi(t)$ according to [10]

$$\phi(t) = \phi_0 + k_{\mathrm{fb}}[\tilde{B}(t) - \tilde{B}_0], \tag{5}$$

$$\tilde{B}(t) = \frac{1}{S}\int_s v\mathrm{d}s, \tag{6}$$

where ϕ_0 is constant ($=0.01$). The integral $\tilde{B}(t)$ takes into account the effect of the average wave activity in the square-shaped sensory domain S. The constant $\tilde{B}_0$ refers to this integral averaged over one period of a spiral placed in the domain center with constant production term $\phi(t) = \phi_0$.

Fig. 2a shows the result of calculations based on Eqs. (3)–(6) with $d = \lambda$ (41 s.u.) and $k_{\mathrm{fb}} = 0.1$. The spiral core was initially located at the center of the sensory domain. Switching on the feedback control induces the drift of the spiral core first outwards from the center and then along a square-shaped trajectory, in good agreement with the experimental results (Fig. 1b). In the parts of the trajectory labeled 1 and 4 the center of the core drifts approximately along a straight line. In part 2 the trajectory starts to bend and to slow down and then turns by 90° in part 3. Corresponding changes in the illumination intensity $\phi(t)$ are shown in Fig. 2b. The feedback algorithm is turned on at $t = 20$ (after about 3 rotations) resulting in large amplitude oscillations of the ϕ values. To show a slight shift in the phase of this oscillation, black dots have been plotted on the abscissa at an interval equal to the oscillation period measured at the part of the trajectory labeled 1. Using these 'stroboscopic' dots, the phase shift, for example, between points labeled 1 and 4 can be determined as 0.54π, which agrees well with the angle difference of the drift directions (90°) at points 1 and 4 of the square-shaped trajectory in Fig. 2a.

The oscillations in $\phi(t)$ are due to corresponding changes of the value of the integral in Eq. (6), which we analyze by considering unperturbed spirals (without feedback) placed inside and outside the quadratic sensory domain. The location of the spiral tip is indicated by black circles labeled with letters P–S, as indicated in the quadratic insert of Fig. 2c. These black circles depict

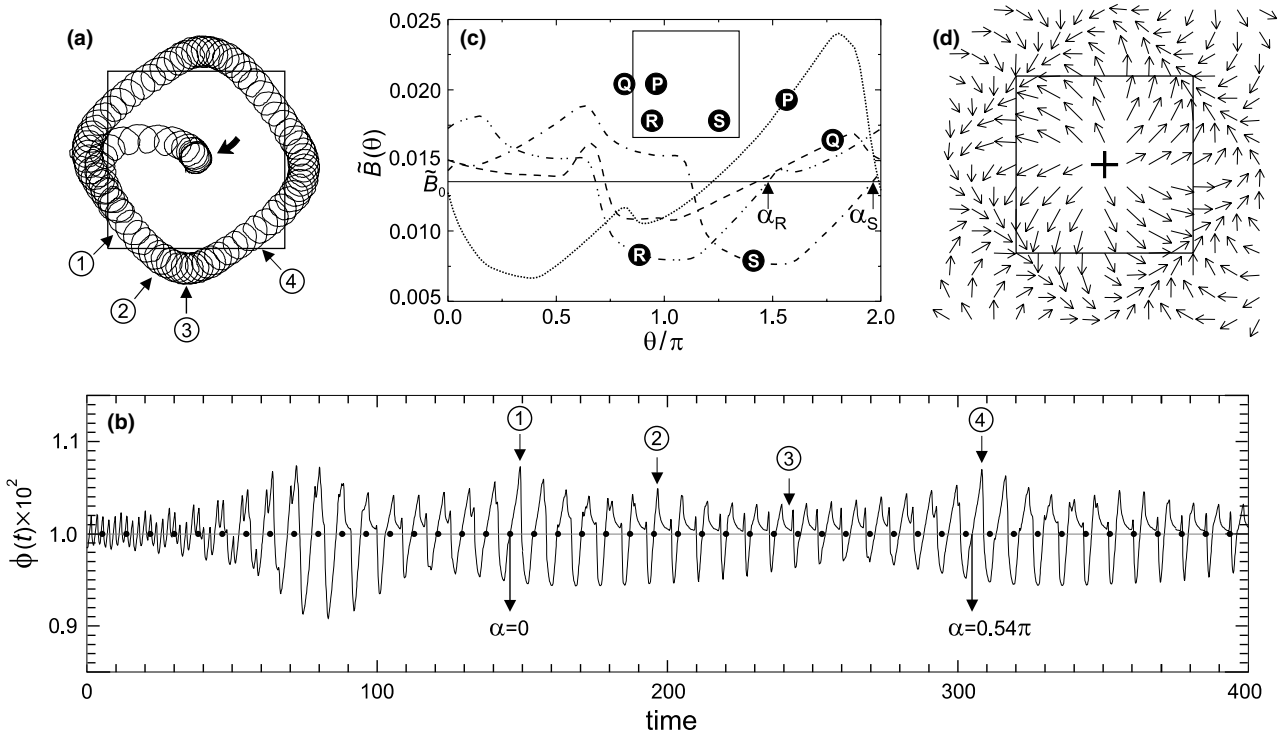

Fig. 2. Spiral wave simulated by Eqs. (3)–(6) under feedback control derived from a square domain with $d = \lambda$. The computations were performed by the explicit Euler method, using a five-point approximation of the Laplacian on a 384×384 array with a grid spacing $\Delta x = 0.5$ and time step triangle $t = 0.001$. (a) Trajectory of spiral wave tip under a feedback control with $k_{\mathrm{fb}} = 0.10$. (b) Value of $\phi(t)$ corresponding to the trajectory in (a). The feedback was switched on at time $= 20$. α is the rotation phase. (c) Analysis of integral (Eq. (6)) as a function of the rotation angle θ of the spiral wave (without feedback) for different locations of the spiral wave core. Each curve is labeled by letters that correspond to those in the square domain (inset) and indicate the location of the spiral core. $\tilde{B}_0$ is the average value of $\tilde{B}(\theta)$ for one rotation of a spiral placed at the domain center. Rotation phases given by arrows are: $\alpha_R = 1.48$, $\alpha_S = 1.97$. (d) Flow map of spiral core trajectory. Arrows indicate the velocity and the direction of the drift. Distance between data points is $1/8\lambda$. The direction of each vector is determined from the difference between the phase of $\tilde{B}$ at that point (arrow tail) and a reference phase (in this case $\pi/4$). Its modulus is calculated as the integral of $|\tilde{B}(\theta)-\tilde{B}_0|$ over one period of the rotation angle θ.

the locations of the spiral core along the trajectory in Fig. 2a. For example, points R and S in the insert correspond to the parts of the trajectory in Fig. 2a, labeled 1 and 4, respectively.

The $\tilde{B}$-values are calculated and plotted in Fig. 2c for one rotation of the spiral ($0 \leqslant$ rotation angle $\theta \leqslant 2\pi$), without feedback. Here, $\tilde{B}$ can be written as a function of the rotation angle $\theta(t)$, which is proportional to time t, i.e. $\tilde{B} = \tilde{B}(\theta)$. The horizontal line in this graph corresponds to $\tilde{B}_0$, as specified in the caption. Curves $\tilde{B}(\theta)$ oscillate with different shape and amplitude for different locations P–S. Considering the extrema of these curves $\tilde{B}(\theta)$, their high values at location P result in a large perturbation and therefore, a fast drift of the spiral wave core, as observed in Fig. 2a. Around location Q, corresponding to one of the corners of the square-shaped trajectory in Fig. 2a, the values of these extrema drop, therefore, the drift around the corners is slow. In order to explain the direction of the drift, the phase of curve $\tilde{B}(\theta)$ must be characterized. Note that all shown curves cross the reference line, $\tilde{B}(\theta) = \tilde{B}_0$, with a positive slope only once during a rotation period. In order to further characterize these curves, the value of the rotation angle at the intersections is defined as the rotation phase α. One can see that the shapes of the $\tilde{B}(\theta)$ curves at locations R and S (with drift directions that are perpendicular to each other) are similar, but their phases differ by about 0.5π (compare α_R and α_S in Fig. 2c). This corresponds well to the phase shift of 0.54π in the feedback signal in parts 1 and 4 of Fig. 2b.

For a more detailed analysis, the local values of $\tilde{B}(\theta) = \tilde{B}_{x,y}(\theta)$ were determined on a finer grid of core locations (x, y). This provides the possibility to construct a flow map shown in Fig. 2d. As described in the caption, this flow map is based on phases representing the drift directions. The integral of $|\tilde{B}(\theta)–\tilde{B}_0|$ over one period is taken as a measure for the magnitude of the perturbation and represents the drift velocity. Most of the flow vectors are attracted towards a square trajectory, on which they are caught in a counterclockwise motion, in agreement with the observed attractor in Fig. 2a.

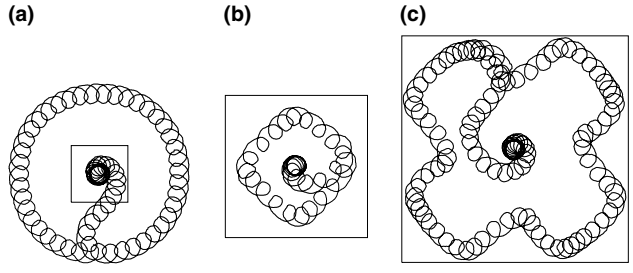

Fig. 3. Simulation results of the spiral wave dynamics under a feedback control derived from different sizes of the domain: (a) $d = 0.5\lambda$, $k_{fb} = 0.10$, (b) $d = 1.25\lambda$, $k_{fb} = 0.20$, and (c) $d = 2\lambda$, $k_{fb} = 0.50$. Trajectories (a) and (b) correspond to experiments shown in Fig. 1a and c, respectively.

The dynamics of such an attractor changes with the size of the integration domain. For a rather small domain ($d = 0.5\lambda$) one obtains a circular attractor (Fig. 3a), similar to that of Fig. 1a. Here, the four-fold geometry of the sensory domain is not reflected in the shape of the trajectory. For domains larger than the spiral wavelength, the size of the attractor decreases, as shown in Fig. 3b where $d = 1.25\lambda$. The 90° turns of the drift direction close to the virtual walls agree with the experimental observation (Fig. 1b). An interesting cross-shaped trajectory is created by further increasing the domain (Fig. 3c).

Our experimental and numerical results demonstrate that the considered nonlocal feedback algorithm is highly efficient to control spiral wave dynamics. The method can be transferred to control such dynamics in other types of spatially extended systems, e.g. in cardiac [19] and neuronal tissue [20] or in the context of intracellular calcium dynamics [21]. The size and shape of a sensor by which we collect information about the activity level of a dynamical system turns out to be crucial and decisive on determining the size and shape of the spatio-temporal attractor governing the behaviour of the system under feedback control.

Acknowledgements

The authors acknowledge the contribution of R. Csillag to the preliminary experiments and thank U. Storb for useful discussions. O.K., S.K. and C.U. thank the Postgraduate Education and Research Program in Chemistry funded by the Royal Thai Government for financial support. O.K. thanks the Thailand Research Fund and V.G. thanks OTKA T038071 for financial support.

References

[1] H.G. Schuster (Ed.), Handbook of Chaos Control, Wiley-VCH, Weinheim, 1999.
[2] K. Pyragas, Phys. Rev. E 66 (2002) 26207.
[3] S. Jakubith, H.H. Rotermund, W. Engel, A. von Oertzen, G. Ertl, Phys. Rev. Lett. 65 (1990) 3013.
[4] M. Kim, M. Bertram, M. Pollmann, A. von Oertzen, A.S. Mikhailov, H.H. Rotermund, G. Ertl, Science 292 (2001) 1357.
[5] A.T. Winfree, Science 175 (1972) 634.
[6] A.L. Lin, M. Bertram, K. Martinez, H.L. Swinney, A. Ardelea, G.F. Carey, Phys. Rev. Lett. 84 (2000) 4240.
[7] K.I. Agladze, V.A. Davydov, A.S. Mikhailov, JETP Lett. 45 (1987) 767.
[8] O. Steinbock, V.S. Zykov, S.C. Müller, Nature 366 (1993) 322.
[9] S. Grill, V.S. Zykov, S.C. Müller, Phys. Rev. Lett. 75 (1995) 3368.
[10] V.S. Zykov, A.S. Mikhailov, S.C. Müller, Phys. Rev. Lett. 78 (1997) 3398.
[11] T. Sakurai, E. Mihaliuk, F. Chirila, K. Showalter, Science 296 (2002) 2009.

[12] O. Kheowan, V.S. Zykov, O. Rangsiman, S.C. Müller, Phys. Rev. Lett. 86 (2001) 2170.
[13] O. Kheowan, C.K. Chan, V.S. Zykov, O. Rangsiman, S.C. Müller, Phys. Rev. E 64 (2001) 35201.
[14] V.S. Zykov, G. Bordiougov, H. Brandtstädter, I. Gerdes, H. Engel, Phys. Rev. Lett. 92 (2004) 18304.
[15] W. Jahnke, A.T. Winfree, J. Bifur. Chaos 1 (1991) 445.
[16] H.J. Krug, L. Pohlmann, L. Kuhnert, J. Phys. Chem. 94 (1990) 4862.
[17] V. Gáspár, Gy. Bazsa, M.T. Beck, Z. Phys. Chem. (Leipzig) 264 (1983) 43.
[18] T. Yamaguchi, L. Kuhnert, Zs. Nagy-Ungvarai, S.C. Müller, B. Hess, J. Phys. Chem. 95 (1991) 5831.
[19] J.M. Davidenko, A.V. Pertsov, R. Salomonsz, W. Baxter, J. Jalife, Nature (London) 355 (1992) 349.
[20] M. Dahlem, S.C. Müller, Exp. Brain Res. 115 (1997) 319.
[21] M. Falcke, Y. Li, J.D. Lechleiter, P. Camacho, Biophys. J. 85 (2003) 1474.